

Molecule-Based Magnets: Ferro- and Antiferromagnetic Interactions in Nickel(II) Cyclohexasiloxanolate Sandwich Complexes

Andrea Cornia,^{1a} Antonio C. Fabretti,^{*1a}
Dante Gatteschi,^{*1b} Gyula Pályi,^{1a} Eva Rentschler,^{1b}
Olga I. Shchegolikhina,^{1c} and Alexandr A. Zhdanov^{1c}

Dipartimento di Chimica, Università di Modena, via G. Campi 183, 41100 Modena, Italy, Dipartimento di Chimica, Università di Firenze, via Maragliano 75/77, 50144 Firenze, Italy, and A. N. Nesmeyanov Institute of Organoelement Compounds (INEOS), 28 Vavilov St., Moscow, Russia

Received March 17, 1995

Introduction

Synthetic and theoretical efforts aimed to find new molecule-based magnetic compounds represent one of the challenges in current fundamental and materials chemistry research.² Such substances include pure organic compounds,³ transition-metal complexes,⁴ and transition metal complexes coupled to organic radicals.⁵

The use of functionalized organic polymers as ligands has been recognized as a new route to materials combining the mechanical properties of the polymeric matrix and the electronic properties of the metal ions.⁶ However, it is in principle possible to use finite-size functionalized oligomers in order to synthesize large metal ion clusters. These systems can be investigated with

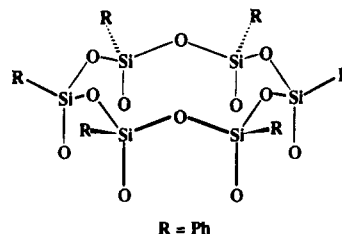


Figure 1. The cyclohexaphenylsiloxanolate, $(\text{PhSiO}_2)_6^{6-}$, ion.

the aim to discover the conditions under which the transition from simple paramagnetic to bulk magnetic behavior can be observed.^{7,8}

The binding properties of polyorganosiloxanates toward transition-metal ions have been investigated by one of our groups, but the resulting polymeric compounds were extremely difficult to characterize due to their amorphous nature.⁹ On the other hand, oligomeric organosiloxanates^{10–16} form metal ion clusters which can be isolated as crystalline phases and structurally characterized. Some mono- and dinuclear complexes have been studied by Fehér's group.¹¹

Cyclic oligomers yield unusual sandwich-type complexes which recently have been investigated as models for silica-supported transition metal catalysts.^{12–16}

Several structurally similar complexes containing the ligand cyclohexaphenylsiloxanolate, $(\text{PhSiO}_2)_6^{6-}$ (Figure 1), and different transition-metal ions have been synthesized. The six pendant "olate" groups of cyclohexaphenylsiloxanolate coordinate metal ions generally acting as bridges between different metal centers. Cyclosiloxanolate ligands can enclose in a cage up to 8 metal ions^{13–16} without direct metal–metal bonds. In the center of the cage additional anions, such as Cl^- , OH^- , and O^{2-} , can be found.

* To whom the correspondence should be addressed.

- (1) (a) Università di Modena. (b) Università di Firenze. (c) INEOS.
- (2) (a) Miller, J. S.; Dougherty, D. A. Proceedings of the Symposium on Ferromagnetic and High Spin Molecular Based Materials. *Mol. Cryst. Liq. Cryst.* **1989**, 176. (b) Gatteschi, D.; Kahn, O.; Miller, S. J.; Palacio, F. *Magnetic Molecular Materials*; NATO ASI Ser.; Kluwer: Dordrecht, The Netherlands, 1991; Vol. 198. (c) Iwamura, H.; Itoh, K.; Kinoshita, M. Proceedings of the International Symposium on the Chemistry and Physics of Molecular Based Magnetic Materials. *Mol. Cryst. Liq. Cryst.* **1993**, 232.
- (3) (a) Tamura, M.; Nakazawa, Y.; Shiomi, D.; Nozawa, K.; Hosokoshi, Y.; Ishikawa, M.; Takahashi, M.; Kinoshita, M. *Chem. Phys. Lett.* **1991**, 186, 401. (b) Nakazawa, Y.; Tamura, M.; Shirakawa, N.; Shiomi, D.; Takahashi, M.; Kinoshita, K.; Ishikawa, M. *Phys. Rev. B* **1992**, 46, 8906. (c) Chiarelli, R.; Novak, M. A.; Rassat, A.; Tholence, J. L. *Nature* **1993**, 363, 147. (d) Rassat, A. *Mol. Cryst. Liq. Cryst.*, in press. (e) Caneschi, A.; Ferraro, F.; Gatteschi, D.; le Lirzin, A.; Rentschler, E. *Inorg. Chim. Acta*, in press. (f) Caneschi, A.; Ferraro, F.; Gatteschi, D.; le Lirzin, A.; Novak, M. A.; Rentschler, E.; Sessoli, R. *Adv. Mater.*, in press.
- (4) Selected recent references: (a) Stumpf, H. O.; Pei, Y.; Kahn, O.; Sletten, J.; Renard, J. P. *J. Am. Chem. Soc.* **1993**, 115, 6738. (b) Ouahab, L.; Pei, Y.; Grandjean, D.; Kahn, O. *Science* **1993**, 261, 447. (c) Mallah, T.; Thiébaud, S.; Verdager, M.; Veillet, P. *Science* **1993**, 262, 1554. (d) Ohba, M.; Tamaki, H.; Matsumoto, N.; Okawa, H. *Inorg. Chem.* **1993**, 32, 5385. (e) Wesolek, M.; Meyer, D.; Osborn, J. A.; deCian, A.; Fischer, J.; Derory, A.; Legoll, P.; Drillon, M. *Angew. Chem., Int. Ed. Engl.* **1994**, 33, 1592. (f) Decurtins, S.; Schmale, H. W.; Schneuwly, P.; Gütlich, P. *J. Am. Chem. Soc.* **1994**, 116, 9521. (g) Godfrey, S. M.; McAuliffe, C. A.; Pritchard, R. G. *J. Chem. Soc., Chem. Commun.* **1994**, 45. (h) Amoroso, A. J.; Maher, J. P.; McCleverty, J. A. *J. Chem. Soc., Chem. Commun.* **1994**, 1273. (i) Mathoniere, C.; Carling, S. G.; Yusheng, D.; Day, P. *J. Chem. Soc., Chem. Commun.* **1994**, 1551. (j) Blake, A. J.; Grant, C. M.; Parsons, S.; Rawson, J. M.; Winpenny, R. E. P. *J. Chem. Soc., Chem. Commun.* **1994**, 2363. (k) Caneschi, A.; David, L.; Ferraro, F.; Gatteschi, D.; Fabretti, A. C. *Inorg. Chim. Acta* **1994**, 217, 7.
- (5) Recent leading references: (a) Caneschi, A.; Gatteschi, D.; Rey, P.; Sessoli, R. *Inorg. Chem.* **1991**, 30, 3936. (b) Benelli, C.; Caneschi, A.; Gatteschi, D.; Sessoli, R. *Inorg. Chem.* **1993**, 32, 4797. (c) Oshio, H. *Inorg. Chem.* **1993**, 32, 4123.
- (6) Wan, M.; Li, J.; Auric, P.; LeCaër, G.; Malaman, B.; Ressouche, E. *Solid State Commun.* **1994**, 89, 999 and references therein.
- (7) (a) Caneschi, A.; Cornia, A.; Lippard, S. J. *Angew. Chem., Int. Ed. Engl.* **1995**, 34, 467. (b) Heath, S. L.; Powell, A. N. *Angew. Chem., Int. Ed. Engl.* **1992**, 31, 191. (c) Taft, K. L.; Papaefthymiou, G. C.; Lippard, S. J. *Inorg. Chem.* **1994**, 33, 1510. (d) Taft, K. L.; Papaefthymiou, G. C.; Lippard, S. J. *Science* **1993**, 259, 1302.
- (8) (a) Gatteschi, D. *Adv. Mater.* **1994**, 6, 635. (b) Papaefthymiou, G. C. *Phys. Rev. B* **1992**, 46, 10366. (c) Delfs, C. D.; Gatteschi, D.; Pardi, L.; Sessoli, R.; Wieghardt, K.; Hanke, D. *Inorg. Chem.* **1993**, 32, 3099.
- (9) (a) Levitskii, M.; Zhdanov, A.; Shchegolikhina, O. I.; Stukan, R.; Knizhnik, A.; Kolbanovskii, A.; Buchachenko, A.; Diakonov, A. *Mol. Cryst. Liq. Cryst.* **1989**, 176, 523. (b) Zhdanov, A. A.; Levitskii, M. M.; Diakonov, A. Yu.; Shchegolikhina, O. I.; Kolbanovskii, A. D.; Stukan, R. A.; Knizhnik, A. G.; Buchachenko, A. L. *Izv. Akad. Nauk SSSR, Ser. Khim.* **1989**, 2512. (c) Zhdanov, A. A.; Buchachenko, A. L.; Shchegolikhina, O. I.; Stukan, R. A.; Knizhnik, A. G.; Levitskii, M. M. *Izv. Akad. Nauk SSSR, Ser. Khim.* **1991**, 606. (d) Zhdanov, A. A.; Buchachenko, A. L.; Diakonov, A. Yu.; Shchegolikhina, O. I.; Levitskii, M. M. *Izv. Akad. Nauk SSSR, Ser. Khim.* **1991**, 778.
- (10) (a) Fehér, F. J.; Newman, D. A.; Walzer, J. F. *J. Am. Chem. Soc.* **1989**, 111, 1741. (b) Darr, J. A.; Drake, S. R.; Williams, D. J.; Slawin, A. M. Z. *J. Chem. Soc., Chem. Commun.* **1993**, 866. (c) Mottevali, M.; Shah, D.; Sullivan, A. C. *J. Chem. Soc., Dalton Trans.* **1993**, 2849.
- (11) (a) Fehér, F. J.; Gonzales, S. L.; Ziller, J. W. *Inorg. Chem.* **1988**, 27, 3440. (b) Fehér, F. J.; Walzer, J. F. *Inorg. Chem.* **1990**, 29, 1604. (c) Edelmann, F. T. *Angew. Chem., Int. Ed. Engl.* **1992**, 31, 600.
- (12) Ovchinnikov, Yu. E.; Shklover, V. E.; Struchkov, Yu. T.; Levitskii, M. M.; Zhdanov, A. A. *J. Organomet. Chem.* **1988**, 347, 253.
- (13) Shchegolikhina, O. I.; Zhdanov, A. A.; Igonin, V. A.; Ovchinnikov, Yu. E.; Shklover, V. E.; Struchkov, Yu. T. *Metalloorg. Khim.* **1991**, 4, 74.
- (14) Levitskii, M. M.; Shchegolikhina, O. I.; Zhdanov, A. A.; Igonin, V. A.; Ovchinnikov, Yu. E.; Shklover, V. E.; Struchkov, Yu. T. *J. Organomet. Chem.* **1991**, 401, 199.
- (15) Igonin, V. A.; Shchegolikhina, O. I.; Lindeman, S. V.; Levitskii, M. M.; Struchkov, Yu. T.; Zhdanov, A. A. *J. Organomet. Chem.* **1992**, 423, 351.
- (16) Igonin, V. A.; Lindeman, S. V.; Potekhin, K. A.; Shklover, V. E.; Struchkov, Yu. T.; Shchegolikhina, O. I.; Zhdanov, A. A.; Razumovskaya, I. V. *Metalloorg. Khim.* **1991**, 4, 790.

Table 1. Crystal Data and Experimental Parameters for $\text{Na}[(\text{PhSiO}_2)_6\text{Ni}_6(\text{PhSiO}_2)_6\text{Cl}]\cdot 12\text{CH}_3\text{OH}\cdot\text{H}_2\text{O}$ (**2**)^a

chem. formula	$\text{Ni}_6\text{NaC}_{84}\text{H}_{110}\text{O}_{37}\text{Si}_{12}\text{Cl}$	fw	2459.38
a	13.791(5) Å	space group	$P\bar{1}$ (No. 2)
b	15.428(5) Å	T	160 K
c	15.488(4) Å	λ	0.710 69 Å
α	60.42(2)°	ρ_{calcd}	1.47 g cm ⁻³
β	83.46(3)°	μ	11.8 cm ⁻¹
γ	72.07(3)°	$R(F_o)$	0.055
V	2724(2) Å ³	$R_w(F_o)$	0.060
Z	1		

$$^a R = \frac{\sum ||F_o| - |F_c||}{\sum |F_o|}; R_w = \frac{\sum w^{1/2} ||F_o| - |F_c||}{\sum w^{1/2} |F_o|}; w = 3.11/[\sigma^2(|F_o|) + 5 \times 10^{-4}|F_o|^2].$$

Table 2. Selected Interatomic Distances (Å) and Angles (deg) for $\text{Na}[(\text{PhSiO}_2)_6\text{Ni}_6(\text{PhSiO}_2)_6\text{Cl}]\cdot 12\text{CH}_3\text{OH}\cdot\text{H}_2\text{O}$ (**2**)^a

Ni(1)–Ni(2)	2.863(1)	Ni(2)–Ni(3)	2.861(1)
Ni(1)–Ni(3')	2.845(1)	Ni(1)–Cl	2.831(1)
Ni(2)–Cl	2.819(1)	Ni(3)–Cl	2.918(1)
Ni(1)–O(1)	2.025(2)	Ni(1)–O(2)	2.011(3)
Ni(1)–O(5')	2.043(2)	Ni(1)–O(6')	2.029(3)
Ni(1)–O(13)	2.056(5)	Ni(2)–O(1)	2.037(4)
Ni(2)–O(2)	2.031(3)	Ni(2)–O(3)	2.023(3)
Ni(2)–O(4)	2.007(4)	Ni(2)–O(14)	2.065(3)
Ni(3)–O(3)	2.012(4)	Ni(3)–O(4)	2.000(3)
Ni(3)–O(5)	2.030(3)	Ni(3)–O(6)	2.028(3)
Ni(3)–O(15)	2.069(4)		
Ni(3')–Ni(1)–Ni(2)	121.20(3)	Ni(3)–Ni(2)–Ni(1)	121.58(2)
Ni(1')–Ni(3)–Ni(2)	117.20(3)	Ni(2)–Cl–Ni(1)	60.90(2)
Ni(1)–Cl–Ni(3)	120.69(2)	Ni(2)–Cl–Ni(3)	59.79(2)
O(2)–Ni(1)–O(1)	80.6(1)	O(2)–Ni(1)–O(6')	169.9(2)
O(2)–Ni(1)–O(5')	97.8(1)	O(2)–Ni(1)–O(13)	100.6(2)
O(1)–Ni(1)–O(6)	99.6(1)	O(1)–Ni(1)–O(5')	170.7(2)
O(1)–Ni(1)–O(13)	95.5(1)	O(6')–Ni(1)–O(5')	80.3(1)
O(6')–Ni(1)–O(13)	89.4(2)	O(5')–Ni(1)–O(13)	93.9(1)
O(4)–Ni(2)–O(3)	79.9(1)	O(4)–Ni(2)–O(2)	99.6(1)
O(4)–Ni(2)–O(1)	168.6(1)	O(4)–Ni(2)–O(14)	94.0(1)
O(3)–Ni(2)–O(2)	168.9(1)	O(3)–Ni(2)–O(1)	98.4(1)
O(3)–Ni(2)–O(14)	99.1(1)	O(2)–Ni(2)–O(1)	79.9(1)
O(2)–Ni(2)–O(14)	91.9(1)	O(1)–Ni(2)–O(14)	94.2(1)
O(4)–Ni(3)–O(3)	80.4(1)	O(4)–Ni(3)–O(6)	97.0(1)
O(4)–Ni(3)–O(5)	166.3(1)	O(4)–Ni(3)–O(15)	100.6(1)
O(3)–Ni(3)–O(6)	167.0(1)	O(3)–Ni(3)–O(5)	98.9(1)
O(3)–Ni(3)–O(15)	97.5(2)	O(5)–Ni(3)–O(6)	80.6(1)
O(6)–Ni(3)–O(15)	95.5(2)	O(5)–Ni(3)–O(15)	93.1(2)

^a Numbers in parentheses are estimated standard deviations in the last significant digit. Primed atoms are related to unprimed ones by the symmetry operation 1 – x , – y , 2 – z .

Preliminary studies indicated that some of these complexes are paramagnetic at room temperature.¹⁷ Given our interest in this area, we decided to start a thorough investigation of the magnetic properties of these systems. Here we wish to report the results of an investigation on $\text{Na}_2[(\text{PhSiO}_2)_6\text{Na}_4\text{Ni}_4(\text{OH})_2(\text{O}_2\text{SiPh})_6]\cdot 16\text{Bu}^n\text{OH}$ (**1**)¹⁶ and $\text{Na}[(\text{PhSiO}_2)_6\text{Ni}_6(\text{O}_2\text{SiPh})_6\text{Cl}]\cdot 12\text{CH}_3\text{OH}\cdot\text{H}_2\text{O}$ (**2**).

Experimental Section

Synthesis. Complexes **1** and $\text{Na}[(\text{PhSiO}_2)_6\text{Ni}_6(\text{O}_2\text{SiPh})_6\text{Cl}]\cdot 14\text{Bu}^n\text{OH}$ (**3**) were prepared by following procedures described elsewhere.^{13,16} Pure X-ray-quality crystals of **2** were grown by slow diffusion of methanol vapors into a CH_2Cl_2 solution of compound **3**. Satisfactory analytical data were obtained for all the compounds.

Magnetic Susceptibility Measurements and EPR Spectra. Magnetic susceptibilities of microcrystalline samples were measured by

Table 3. Final Significant Coordinates with Esd's and Equivalent Thermal Parameters for $\text{Na}[(\text{PhSiO}_2)_6\text{Ni}_6(\text{PhSiO}_2)_6\text{Cl}]\cdot 12\text{CH}_3\text{OH}\cdot\text{H}_2\text{O}$ (**2**)

atom	x/a	y/b	z/c	$B_{\text{eq}}, \text{Å}^2$
Ni(1)	0.52618(4)	–0.05684(4)	0.84889(4)	1.66(2)
Ni(2)	0.49577(4)	0.15475(4)	0.80012(4)	1.61(2)
Ni(3)	0.46620(4)	0.21609(4)	0.95023(4)	1.62(2)
Cl(1)	0.5	0.0	1.0	2.39(5)
Si(1)	0.29401(8)	0.09826(8)	0.77056(8)	1.52(3)
Si(2)	0.25878(8)	0.26678(8)	0.82821(8)	1.65(3)
Si(3)	0.24336(8)	0.20535(8)	1.04791(9)	1.82(4)
Si(4)	0.73179(8)	0.02174(8)	0.80035(8)	1.79(4)
Si(5)	0.69419(8)	0.18929(8)	0.86073(8)	1.70(4)
Si(6)	0.68229(8)	0.12839(8)	1.07783(8)	1.61(3)
O(1)	0.5849(2)	–0.0786(2)	1.2258(2)	1.60(9)
O(2)	0.3880(2)	–0.0419(2)	1.2102(2)	1.76(9)
O(3)	0.3791(2)	0.2456(2)	0.8376(2)	1.80(9)
O(4)	0.5741(2)	0.2092(2)	0.8541(2)	1.75(9)
O(5)	0.3634(2)	0.1866(2)	1.0583(2)	2.0(1)
O(6)	0.5613(2)	0.1523(2)	1.0706(2)	1.77(9)
O(7)	0.7685(2)	–0.1942(2)	1.2090(2)	2.0(1)
O(8)	0.2073(2)	0.2438(2)	0.9349(2)	2.1(1)
O(9)	0.2106(2)	0.1001(2)	1.1211(2)	2.3(1)
O(10)	0.7575(2)	0.0918(2)	0.8418(2)	2.2(1)
O(11)	0.7328(2)	0.1620(2)	0.9690(2)	2.0(1)
O(12)	0.7390(2)	0.0042(2)	1.1476(2)	2.0(1)
O(13)	0.4638(3)	0.1030(3)	1.2565(3)	3.2(1)
O(14)	0.4937(3)	–0.2617(3)	1.3463(2)	2.7(1)
O(15)	0.4376(3)	0.3685(3)	0.9197(3)	3.2(1)
Na(1)	0.5119(4)	–0.1505(5)	1.4251(4)	4.7(2)
OH(2)	0.5359(7)	0.851(1)	0.5063(8)	5.6(5)

$$^a B_{\text{eq}} = \frac{1}{3} \sum_i \sum_j B_{ij} a_i^* a_j^* a_i a_j$$

using a Métrologie Ingénierie MS03 SQUID magnetometer in the temperature range 2.3–160 K and 2.6–270 K for compounds **1** and **2**, respectively. An applied field of 0.1 T from 2.3–36 K and 1 T up to 160 K was used for compound **1**, while for compound **2** an applied field of 1 T was used in the whole temperature range. The magnetization of compound **1** was measured at 2.2 K in the field range 0–7 T. The contribution of the sample holder was determined separately in the same temperature range and field. Diamagnetic corrections were estimated from Pascal's constants.

EPR spectra of powdered samples were obtained with a Varian E9 spectrometer operating at X-band frequency, equipped with an Oxford Instruments ESR9 liquid helium continuous flow cryostat.

Least-Squares Calculations. All calculations for the fitting of the magnetic data were performed on RISC and CONVEX220 computers. $R = \sum_i [Y_i^{\text{obs}} - Y_i^{\text{calc}}]^2 / \sum_i [Y_i^{\text{obs}}]^2$ was minimized in the least-squares cycles.

X-ray Data Collection and Structure Refinement. Diffraction data for compound **2** were collected on a CAD4 automatic diffractometer equipped with a low-temperature facility. Selected experimental parameters and crystal data are reported in Table 1. A total of 11 026 reflections were collected in the range $5 \leq 2\theta \leq 52$.

No absorption correction was applied. The structure was solved by direct methods using the *SIR92*^{18a} program, which gave the positions of all non-hydrogen atoms except for the highly disordered solvated methanol molecules. Refinement was carried out with the *SHELX76*^{18b} program package on 8649 reflections with $I > 4.5\sigma(I)$ and 603 parameters. Attempts to obtain a satisfactory model for disorder failed, as demonstrated by the somewhat large residual electron density (1.82 e Å⁻³). The solvated methanol molecules were isotropically refined during several least-squares cycles and then held fixed. All the remaining non-hydrogen atoms were treated anisotropically. Hydrogen atoms were set in calculated positions and refined as riding atoms with $B(\text{H}) = 1.2B_{\text{eq}}(\text{C})$, where C is the parent carbon atom. Selected interatomic distances and angles are gathered in Table 2. Final significant atom coordinates and equivalent thermal parameters are in Table 3. Full listing of crystal data, experimental parameters, final

(17) (a) Gavioli, G.; Battistuzzi, R.; Santi, P.; Zucchi, C.; Pályi, G.; Ugo, R.; Vizi-Orosz, A.; Shchegolikina, O. I.; Pozdniakova, Yu. A.; Lindeman, S. V.; Zhdanov, A. A. *J. Organomet. Chem.* **1995**, *485*, 257. (b) Shchegolikina, O. I.; Pozdniakova, Yu. A.; Lindeman, S. V.; Zhdanov, A. A.; Psaro, R.; Ugo, R.; Gavioli, G.; Battistuzzi, R.; Borsari, M.; Rüffer, T.; Zucchi, C.; Pályi, G. *J. Organomet. Chem.*, submitted for publication.

(18) (a) Altomare, A.; Casciaro, G.; Giacovazzo, C.; Guagliardi, A. J. *Appl. Cryst.* **1994**, *27*, 1045. (b) Sheldrick, G. M. *SHELX76, Program for Crystal Structure Determination*; University of Cambridge: Cambridge, England, 1976.

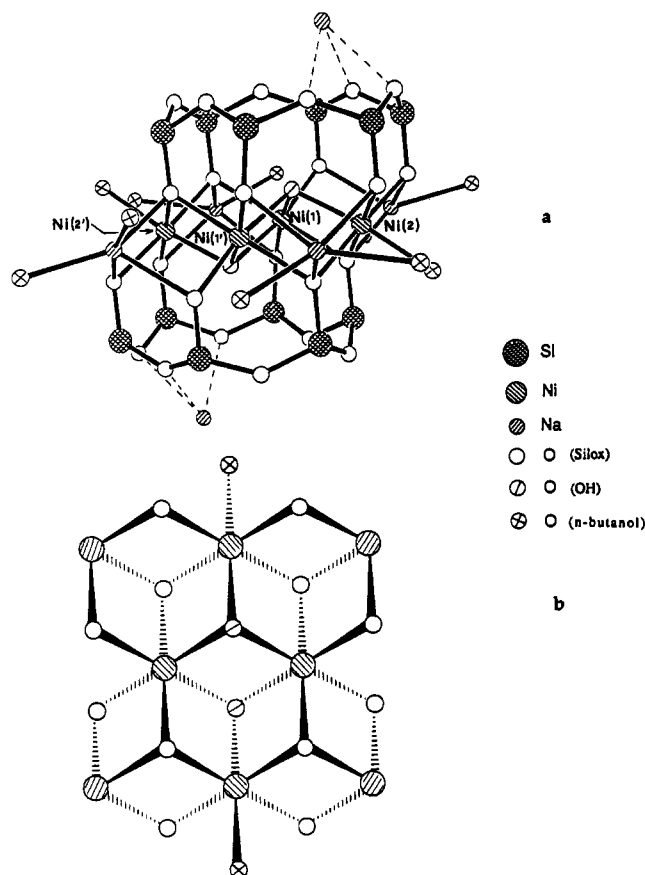


Figure 2. (a) Sketch of the complex core of **1**. The phenyl rings of the cyclohexaphenylsiloxanolate ligands, the alkyl chains of the butanol molecules, and the hydrogen atoms of the OH groups have been omitted for clarity. (b) Simplified view of the structure.

atom positional and thermal parameters, and bond lengths and angles are given in the Supporting Information.

Results and Discussion

Structure of the Complexes. The molecular structure of the tetranuclear nickel(II) complex **1** is shown in Figure 2a.¹⁶ The four nickel(II) ions are hexacoordinated. Each nickel(II) ion is linked to four siloxanolate oxygen atoms. Ni(1) and Ni(1') are further coordinated by two bridging OH⁻ groups, while Ni(2) and Ni(2') are coordinated by one OH⁻ group and one oxygen from a *n*-butanol molecule.

The molecular structure of complex **2** is shown in Figure 3. The nickel ions, which are located at the vertices of an almost regular hexagon, are in tetragonally distorted octahedral surroundings. Adjacent metal ions are bridged by two siloxanolate oxygen ligands, one above and one below the average plane of the hexagon. They occupy the equatorial positions of the metal coordination spheres, the axial positions being occupied by methanol molecules and by the encapsulated μ_6 -chloride ion. The compounds Na[(PhSiO₂)₆Ni₆(O₂SiPh)₆Cl]·14BuⁿOH (**3**)¹³ and Na[(PhSiO₂)₆Ni₆(O₂SiPh)₆Cl]·9EtOH·4H₂O (**4**)¹³ have a similar overall molecular structure, the apical sites of the metals being occupied by *n*-butanol and ethanol ligands, respectively. In all cases the Ni, Si, O skeleton approaches *6/mmm* symmetry. The Ni—O_{eq} and Ni—O_{ax} distances are in the range 1.998–2.044 and 2.054–2.076 Å, respectively, and are found to be close to the Ni—O distance in NiO (2.1 Å). On the other hand, the Ni—Cl bond lengths (2.819–2.918 Å) are apparently elongated, being closer to the sum of the ionic radii of Cl⁻ and Ni²⁺ (3.19 Å) than to the Ni—Cl separation in NiCl₂ (2.47 Å). The angles at the bridging oxygens fall in the range 89.7–91.1°.

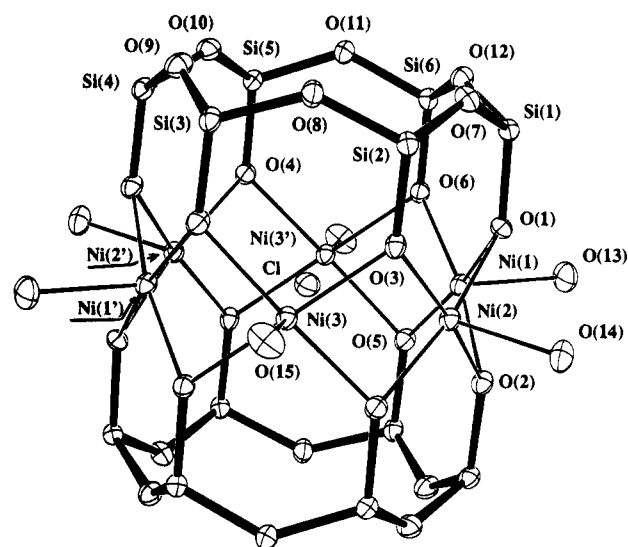


Figure 3. Sketch of the complex core of **2** with thermal vibration ellipsoids (30% probability). The phenyl rings of the cyclohexaphenylsiloxanolate ligands and the methyl groups of the methanol molecules have been omitted for clarity.

Complexes **1** and **2** share one important feature of their metal–oxygen cores: the oxygen donors in the coordination spheres of the metal ions are arranged in two layers, one above and one below the average plane through the metals. The nickel–sodium–oxygen core of complex **1**, in particular, can be easily described as a fragment of a CdI₂-type layered structure (Figure 2b): the oxygen atoms form a cp (close-packing) double layer whose octahedral interstices are occupied by the metal ions. A suitable extension of the layer in a direction perpendicular to the mean plane through the metals leads formally to the NiO fcc lattice. The presence of cp arrays of oxygen atoms indeed represents a fundamental structural feature of several nanoscale polymetallic systems. The possibility to describe the structures of these molecular entities by using concepts developed for extended lattices allows a straightforward rationalization of the structures and may represent a valuable starting point to investigate correlations between structural and physical properties. Furthermore, it may throw light on the aggregation processes which are responsible for the growth of polynuclears, as recently observed in the case of a number of polyiron(II,III) clusters.^{7,19}

Magnetic Properties. The magnetic behavior of complex **1** is shown in Figure 4 as a χT vs T plot. The value of χT increases upon cooling from 5.7 emu·K·mol⁻¹ at 160 K to a maximum of 12.5 emu·K·mol⁻¹ at 8 K. This description corresponds to a pattern of moderate ferromagnetic coupling in which the highest value of χT is consistent with that expected for a spin-aligned ground state arising from the intramolecular interactions between the four Ni(II) ions. An $S = 4$ state of the tetranickel complex, in which all four spins are parallel, corresponds in fact to a χT value of 12.1 (13.2) emu·K·mol⁻¹ for $g = 2.2$ (2.3). Further cooling causes the χT product to decrease, reaching 11.7 emu·K·mol⁻¹ at 2.3 K.

Since the same temperature dependence of χT is observed in low-field measurements, it may be concluded that zero-field-splitting effects are responsible for the decrease of χT below 8

(19) (a) Caneschi, A.; Cornia, A.; Fabretti, A. C.; Gatteschi, D.; Malavasi, W. *Inorg. Chem.*, in press. (b) Lippard, S. J. *Angew. Chem., Int. Ed. Engl.* **1988**, *27*, 344. (c) Lippard, S. J. *Chem. Br.* **1986**, *22*. (d) Hagen, K. S. *Angew. Chem., Int. Ed. Engl.* **1992**, *31*, 1010.

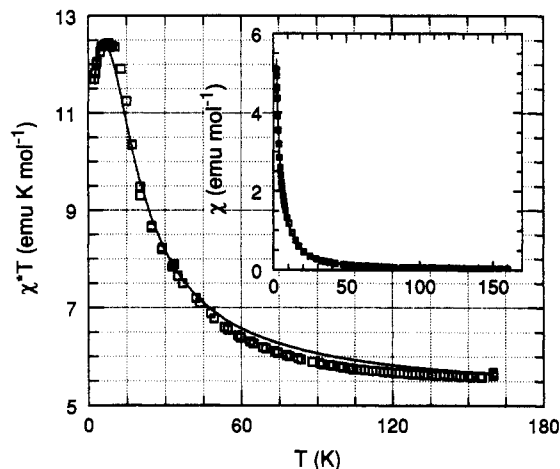


Figure 4. Experimental and calculated temperature dependence of χ and χT for compound **1**. (See text for details.)

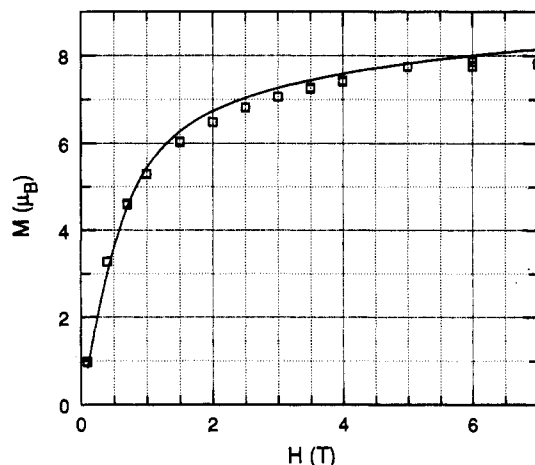


Figure 5. Experimental and calculated field dependence of the magnetization of compounds **1** at 2.2 K (see text for details).

K. In order to confirm this conclusion, the field dependence of the magnetization in the range 0–7 T was checked at 2.2 K (Figure 5). The value of the magnetization at 7 T ($7.8 \mu_B$) is smaller than expected for an $S = 4$ state ($8.8 \mu_B$ for $g = 2.2$). We tried to reproduce the magnetization data assuming that at 2.2 K the ground $S = 4$ state can be considered as well separated from the excited states and that it undergoes zero-field splitting presumably due to single ion contributions. The calculated curve, using the Hamiltonian (1) with $g = 2.2$ and $D = 1.2$

$$H' = -g\mu_B \mathbf{H} \cdot \mathbf{S} + D[S_z^2 - S(S+1)/3] \quad (1)$$

cm^{-1} , is shown in Figure 5. The agreement with the experimental data can be considered as satisfactory.

The experimental χT vs T data have then been fitted using Hamiltonian (2), where \mathbf{S}_i is the spin vector operator localized

$$H = H_{\text{ex}} + H_{\text{Zeem}} + \delta H_{\text{ZFS}} \quad (2)$$

$$H_{\text{ex}} = J_1(\mathbf{S}_1 \cdot \mathbf{S}_2 + \mathbf{S}_1 \cdot \mathbf{S}_2' + \mathbf{S}_1 \cdot \mathbf{S}_2'' + \mathbf{S}_1 \cdot \mathbf{S}_2''') + J_2(\mathbf{S}_1 \cdot \mathbf{S}_1') \quad (3)$$

on $\text{Ni}(i)$, $\delta = 1$ for the ground $S = 4$ state, and $\delta = 0$ for all the other states. The following best-fit parameters have been obtained: $J_1 = -7(1) \text{ cm}^{-1}$, $J_2 = -3(1) \text{ cm}^{-1}$, $g = 2.27(2)$, and $D = 1.0(2) \text{ cm}^{-1}$ with $R = 1.95 \cdot 10^{-2}$.

Although the best-fit values of J_1 and J_2 are subject to large statistical correlations, the ferromagnetic character of the interactions can be unequivocally established.

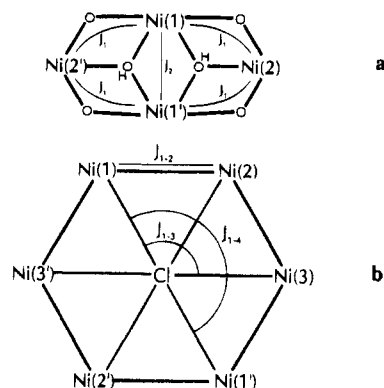


Figure 6. Adopted scheme for the exchange-coupling interactions in compound **1** (a) and **2** (b).

The single quasi-isotropic line at $g \approx 16$ observed in the EPR spectrum of complex **1** at 4.2 K may arise from transitions within the zero-field split $S = 4$ manifold. Considering the molecular structure of the tetranickel complex **1**,¹⁶ the major contribution to J_1 and J_2 is certainly due to superexchange effects through the μ_3 -OH groups and the siloxanolate oxygen ligands rather than to direct overlap of Ni orbitals (Figure 6a). The Ni–Ni separation is larger than 3 Å, therefore longer than in nickel metal (2.44 Å). Implicit in Hamiltonian (3) is the assumption that the interaction between $\text{Ni}(2)$ and $\text{Ni}(2')$ is negligible, since they are far apart from each other and they have no common bridging ligand. As found for other polynuclear nickel(II) complexes showing ferromagnetic intramolecular coupling through oxygen bridges,^{20–22} the Ni–O–Ni angles deviate appreciably from 90° . The angles at the siloxanolate oxygen atoms are 94.8 – 95.8° whereas those at the OH bridges are 99.6 – 100.3° . Our findings, therefore, are in agreement with the theory of Ginsberg *et al.*,²⁰ who predicted that deviations of $\pm 14^\circ$ from 90° can be tolerated before the superexchange pathways lose their predominant ferromagnetic character. Another tetranuclear nickel(II) compound with bridging azido and RO⁻ ligands was recently reported²² to have an $S = 4$ ground state. The bridging angles are 76 and 98° , respectively, and J was found to be -21.3 cm^{-1} .

The magnetic behavior of **2** is shown in Figure 7. The room-temperature value of the χT product ($8.4 \text{ emu} \cdot \text{K} \cdot \text{mol}^{-1}$) agrees with that expected for a system of six uncoupled $S = 1$ spins with a moderately high g value [$7.94(8.64)$ for $g = 2.2(2.3)$]. Upon decreasing temperature χT decreases continuously and goes to zero in the 0 K limit. On cooling down from room temperature, the molar susceptibility increases, passes through a maximum at about 32 K, and then decreases rapidly, pointing at the presence of prevalent antiferromagnetic interactions. This is at first sight surprising, because the geometry of the siloxanolate bridges is not very different in **1** and **2**. Assuming a $6/mmm$ point-group local symmetry for the $[\text{Ni}_6(\text{OR})_{12}\text{Cl}]$ core of **2**, three symmetry-independent exchange-coupling interactions can be envisaged: 1 – 2 type interactions, involving the siloxanolate bridges and the central chloride ligand; 1 – 3 and 1 – 4 type interactions, essentially involving the central chloride ligand only (Figure 6b). Assuming $J_{1-3} = J_{1-4} = J'$ for simplicity, a satisfactory agreement with the experimental χ vs T data can be obtained with $J_{1-2} < 0$ and $J' > 0$, *i.e.* the central μ_6 -chloride ion mediates antiferromagnetic interactions. The

(20) Bertrand, J. A.; Ginsberg, A. P.; Kaplan, R. I.; Kirkwood, C. E.; Martin, R. L.; Sherwood, R. C. *Inorg. Chem.* **1971**, *10*, 240 and references therein.

(21) Gladfelter, W. L.; Lynch, M. W.; Schaefer, W. P.; Hendrickson, D. N.; Gray, H. B. *Inorg. Chem.* **1981**, *20*, 2390.

(22) Ribas, J.; Monfort, M.; Costa, R.; Solans, X. *Inorg. Chem.* **1993**, *32*, 695.

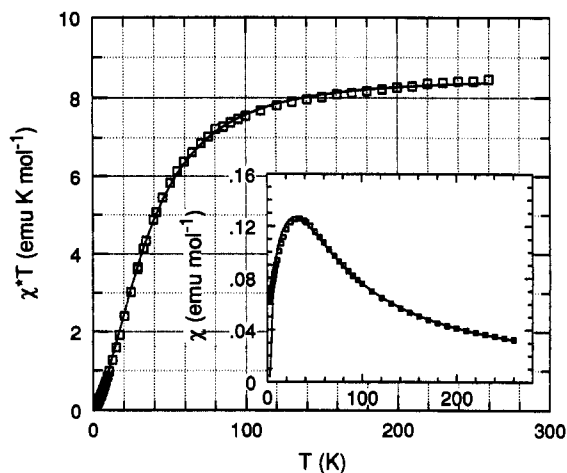


Figure 7. Experimental and calculated temperature dependence of χ and χT for compound **2**. (See text for details.)

resulting best-fit parameters are as follows: $g = 2.38$, $J_{1-2} = -18.6 \text{ cm}^{-1}$, and $J' = 11.8 \text{ cm}^{-1}$ with $R = 2.63 \times 10^{-4}$.

We have therefore shown that the bridging geometry of the siloxanolate oxygen donors in **1** and **2** leads to ferromagnetic intramolecular spin–spin interactions. In complex **2** the encapsulated μ_6 -chloride ion provides sufficient antiferromagnetic pathways for resulting in an $S = 0$ ground state. In complex **1**, on the other hand, the μ_3 -hydroxide ligands are likely to mediate additional ferromagnetic interactions, leading to an $S = 4$ ground state. Therefore the magnetic behavior of the latter compound differs fundamentally from that of the cubic

polymorph of nickel oxide, which is simply a paramagnet.²³ The possible growth of the tetranuclear core of **1** in a direction parallel to the plane of the layer, to yield an octanickel(II) cluster complex, has been demonstrated by X-ray techniques.¹⁴

Our groups intend to continue this line of research since it appears to us that the magnetic behavior of siloxanolate/transition-metal complexes may provide a substantial contribution to the understanding of magnetic coupling phenomena as well as to the tailoring of nanostructured new materials. Furthermore, these compounds might be used as precursors to silica-embedded magnetic materials.

Acknowledgment. Thanks are due to the “Ministero dell’Università e della Ricerca Scientifica e Tecnologica” (MURST) and to the National Research Council (CNR), P. F. Chimica Fine II, of Italy for financial support; we are also grateful to the “Centro Interdipartimentale di Calcolo Automatico ed Informatica Applicata” (CICAIA) of Modena University for computer facilities.

Supporting Information Available: Listings of complete crystal data and experimental parameters (Table S1), final atom positional and equivalent thermal parameters and fractional SOF’s for non-hydrogen atoms (Table S2), bond lengths and angles (Table S3), anisotropic thermal parameters (Table S4), and fractional coordinates and isotropic thermal parameters for hydrogen atoms (Table S5) for complex **2** (9 pages). Ordering information is given on any current masthead page.

IC950320X

(23) Schieber, M. M. *Experimental Magnetochemistry*; North-Holland Publishing Co.: Amsterdam, 1967.